eJSE International

Electronic Journal of Structural Engineering 20(1) 2020

Stochastic Finite Fault Modeling and Simulation of Strong Ground Motion of Mosha Fault in Iran

H. Saffari & A. Roohafzayan, A. Mahdavian
University of Shahid Beheshti, Iran

M. Yari
University of University of Mohaghegh Ardabili

ABSTRACT: This study aims at predicting large earthquakes caused by Mosha fault in Tehran, the capital of Iran with population of more than 13 million people which located alongside active faults. This study uses the EXSIM program to do the finite fault modeling of simulation. Using Geopsy software and programming in MATLAB we evaluated the site effect of 13 station. Using other required parameters of Mosha fault in EXSIM, we gained the artificial strong motions of the stations. Finally, using SeismoSignal and MATLAB software, we depicted the Acceleration -time graph and the semi-logarithm frequency spectrum with "Fourier transform" of each station. we compared the results of the finite fault simulation with Ambraseys attenuation relationship, semi-logarithm frequency spectrum with Fourier transform and spectrum-response graphs of 2009 earthquake in Shahr-e Rey measuring Mw = 4.2. In both cases of comparing meaningful results were found. Finally, in order to generalize the results to the city of Tehran, we evaluated the seismicity using Arc GIS software. The results show that if Mosha fault is activated, east of Tehran is influenced the most. Consequently, it is of high importance to study different ways to reduce the risk of the possible earthquake caused by Mosha fault.

1 INTRODUCTION

Tehran city is the center of Tehran province. In the last population and housing census, more than 13.260.000 people inhabited Tehran, which makes it the largest city in Iran (Statistical Center 2018). Tehran is increasingly growing and needs safe constructions and infrastructures. Due to the inability of the spectrum-response method, analysis and design of the structures are not capable of providing time data about behavior and response of the structure. As a result, most of Building Cod Methods have required dynamic analysis in special cases such as Irregular structures. The ultimate design of important structures such as nuclear power plants, dams, tall buildings, cable bridges, etc., are made based on the time history analysis. It is important for this type of analysis to have the ground motion of the location of the structure. The recorded ground motions are to a great extent reliant on the mechanism, structure, local conditions etc. The suitable ground motion for analyzing each structure are records which have got similar characteristics for each location. Accordingly, considering the low number of recorded and analyzed ground motion, it is difficult, sometimes impossible, to select suitable ground motion based on reality. Due to the differences in geological properties, the records of the occurred earthquakes in other places do not meet the requirements. Regarding the short history of the establishment of Iran Strong Motion Network (most of the data belongs to the last fifty years), the lack of recorded strong motions and their limitations, and the increasing use of dynamic analysis, we need a method that uses the existing ground motion and artificially generated ground motion in which spectrum response of the artificial ground motion matches the design spectrum of the location. There are many ways to produce artificial strong ground motions including random sampling method.

This method is widely used in predicting strong ground motions. It is based on the fact that considering the randomness of the movements, we can combine the suggested models for the earth movements with high frequencies. In the random sampling methods, there are two kinds of stochastic point effect: in the first kind the simulation is based on stochastic point source method and in the second one the simulation is based on the finite fault method. Stochastic point source method is based on the spectrum called ω2 and corner frequency. The spectrum range from the stochastic point source method has been predicted for 0.1 to 2HZ frequencies and a magnitude of more than 4. The stochastic point method can't take into account the key parameters of a big earthquake such as the long time and directional effect. Due to these limitations, the finite fault method was introduced by Hartzell in 1978 (Hartzell 1978). It has been widely accepted in recent years. This method of simulation is suitable and it is widely used in evaluating strong ground motion. As a result, this article uses the finite fault method to simulate the strong ground motion for Mosha fault.

2 REGION OF STUDY

Faults are the stochastic point sources of earthquakes which can be the place of the possible earthquakes in the future. Displacement of faults can influence the structures located on them. Iran is located on the Alps-Himalayas seismic belt. Many parts of the north, center, and south of Iran are influenced by big and small earthquakes. Tehran is located in the southern part of the Alborz range and has many active faults including Mosha fault, the fault of the north of Tehran, The southern-northern Rey fault. Besieged by all these faults, Tehran has the potential to experience many earthquakes. Figure 1 shows Tehran and the faults surrounding it.

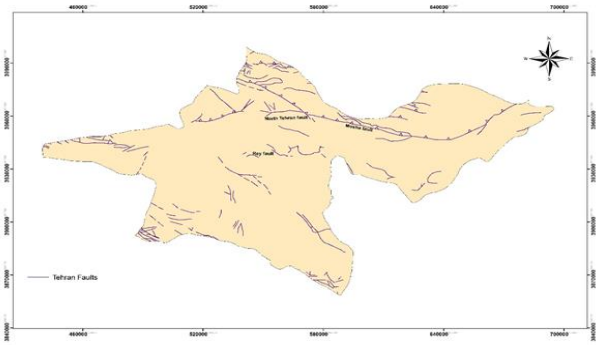

Figure 1. The layout of Tehran faults

Mosha fault is the most dangerous source of earthquakes in Tehran. It is located in Alborz range with a length of 220km, far away from Tehran. The closest bordering distance of Mosha fault is 25km from the northern ridges of Tehran. It has many parts and will influence Tehran more than other places. According to the seismic data, this area has experienced powerful earthquakes in the past including the earthquakes in 1665 AD and 1830 AD, measuring Mw= 6.5 and Mw= 7.1 respectively, which hit at the distance of 77 and 120km away from the north of Tehran respectively. These earthquakes happened in a time period of 165 years. The 1830 earthquake caused a lot of damage to Tehran (Berberian 1994). According to the data, the possibility of a similar earthquake in near future is so high. It is clear that the possible earthquake will cause lots of damages and will stirs up high casualty to Tehran due to the large population and distressed urban areas. For this reason, we have chosen Mosha fault to be studied in this research.

Mosha fault was first called Mosha-Fasham by Dellenbach (Dellenbach 1964) and Tchalenko (Tchalenko and Braud 1974) used the same name. This fault was called Meiygon-Mosha expulsion by Assereto (Assereto 1966). Since Mosha-Fasham fault lies between the two villages, we call it Mosha fault. It is an important long fault which lies between the northern and southern parts of Alborz range. It stretches from east-southeast and west-northwest directions. Mosha fault has got a sinusoidal form on the map. Its slope is always northward between 35 to 70 degrees. It is almost 220km long and stretches from the east of Mosha village to Abyek village in the west. According to the researches, its expulsion occurred before the Jurassic period (Allenbach 1966). The rupture of the middle part of Mosha fault which is the most active part of it (Tatar, Hatzfeld et al. 2012) has been considered as a rupture scenario.

3 FINITE FAULT MODELLING WITH DYNAMIC CORNER FREQUENCY

One of the different ways of evaluating earthquakes by the use of acceleration time series is to simulate the strong ground motion movement. Simulation of this movement plays an important role in estimating different parameters particularly for those parts for which we don't have enough data. The properties of the strong ground motion are of high importance for designing, strengthening, and improving the structures. In the finite fault method, simulation of the movements caused by small earthquakes Caused by subfaults has been suggested as a way for predicting the Near-Fault Ground Motions (Mavroeidis and Papageorgiou 2003).

In this method, the recorded strong motion is the result of the combination of the earthquake source (E), path (P), the site effect (G), and instrument or type of motion (I) (Boore 2003) which is presented in the frequency realm, as:

$$Y(M_0 \times R \times f) = E(M_0 \times R)P(R \times f)G(f)I(f) \quad (1)$$

Motazedian and Atkinson have presented a suitable method to simulate earthquake strong motions in the form of the EXSIM program (Motazedian and Atkinson 2005). This method uses the random sampling method of finite fault based on the dynamic corner frequency. In order to consider the pulse-like ground motions, the mathematical model of a pulse model, Papageorgiou and Mavroeidis (Mavroeidis and Papageorgiou 2003) were used. In this method, the fault is divided into elements and a subevent is simulated for each element. Finally, in the strong motions-recording station, the general strong motions are made by adding the effects of subevents. In this method, a large fault is divided into N subfaults. Each of these subfaults is considered as a small stochastic point. Strong ground motions in each subfault is calculated using the random sampling method of the stochastic point. Then, in the desired point with a suitable time delay, they are added to calculate the Strong ground motions in the whole area.

$$a(t) = \sum_{j=1}^{nw} \sum_{i=1}^{nl} a_{ij}(t + \Delta t_{ij}) \quad (2)$$

Where nw and nl are the number of subfaults along the main part of the fault. As a result, nl×nw and $a_{ij}(t)$ are the time delay of radiated wave from ijth subfault which reaches the desired point. a_{ij} (t) is the calculated amount based on the random sampling method. The Acceleration spectrum of the i_{th} subfault is defined as:

$$A_{ij}(f) = \left\{\frac{CM_{0ij}(2\pi f)^2}{\left[1+\left(f_{ij}^2\right)\right]}\right\} \times \left\{\frac{\exp(-\pi f k)\exp\left(-\frac{\pi f R_{ij}}{Q\beta}\right)}{R_{ij}}\right\} \quad (3)$$

In this relation, M_{0ij},F_{ij}, R_{ij} are seismic moment, corner frequency and the distance of ij_{th} subfault from the main fault respectively. $C=R_{\theta\emptyset}F\times V/4\pi\rho\beta^3$ in which R_(θØ) is radiation pattern which is approximately 0.55 for shear waves. F is the amplification factor of the surface layer which is 2; V is the participation of two shear waves of SV and SH which is 0.71; ρ is density and β is the speed of the shear wave. $\exp(-\pi f k)$is a high-cut filter to model near surface kappa effects: this is the commonly observed rapid spectral decay at high frequencies (Anderson and Hough 1982). Q(f), is inversely related to anelastic attenuation. The implied 1/R geometric attenuation term is applicable for body-wave spreading in a whole space (Motazedian and Atkinson 2005).

4 METHODOLOGY

The required parameters for the simulation of the finite fault modeling include the geometry of the fault, the describing parameters of zonal damping, and the data related site effect.

4.1 *Geometry of the fault*

Using the relations provided by Wells and Coppersmith (Wells and Coppersmith 1994), the geometry of the fault is determined by the following formulas:

$$\log(RLD) = a \times b \times m \quad a = -2.45 \quad b = 0.9 \quad (4)$$
$$\log(Rw) = a \times b \times m \quad a = -1.01 \quad b = 0.32 \quad (5)$$

In these relations, RLD, is the subsurface rupture length and Rw, is the downdip rupture width (Wells and Coppersmith 1994). a and b are stable parameters gained empirically. Based on this, Mosha fault dimensions are 78km in length, along the rupture and its width is 23km.

4.2 *Site effect*

In order to evaluate the Site effect, the Nakamura method is used to eliminate the source effects (Nakamura 1989). This method is based on the modification of the transfer function of the location. In this method, the transfer function is gained by dividing the microtremor spectrum of the horizontal to the vertical parameters. Most often the ratio of the horizontal parameter spectrum to the vertical parameter in resonance frequency results in the shear wave frequency. Based on this, dividing the horizontal parameter to the vertical parameter allows the removal of stochastic-like effects of the Rayleigh wave. Nakamura method is a practical method to determine the features of the earth movements (Nakamura 1989). Based on this, we selected 13 stations as shown in figures 2.

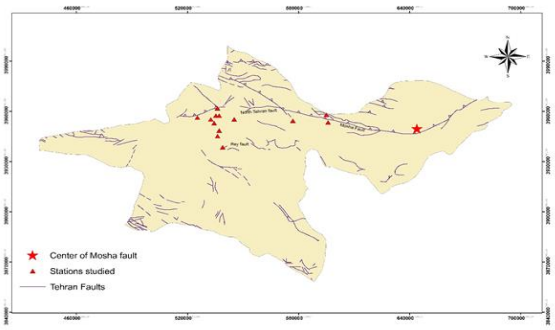

Figure 2. The evaluated station

Using Geopsy and MATLAB software, the amplification factor of the location was calculated in different stations. In this research, using the strong ground motions of different earthquakes, the site effect parameters used to determine the site effect after applying the base line filters. These earthquakes include: Tehran (February 17, 2006), Tehran (September 8, 2006), Tehran (December 25, 2006), Tehran (February 26, 2007), Tehran (March 2, 2007), Tehran (February 10, 2008), Mazandaran (June 29, 2008), Golestan (August 16, 2009), Tehran (December 17, 2009), Tehran (January 20, 2010).
Figures 3-15 show the site effect of the selected stations.

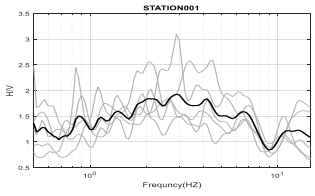

Figure 3. Site effect of station 001

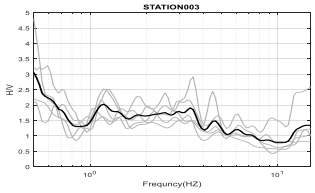

Figure 4. Site effect of station 003

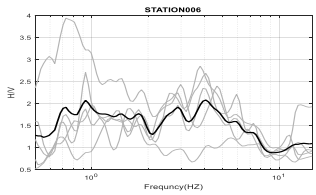

Figure 5. Site effect of station 006

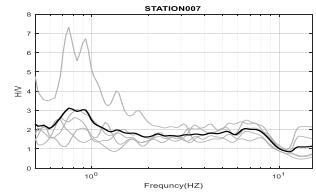

Figure 6. Site effect of station 007

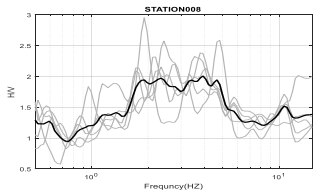

Figure 7. Site effect of station 008

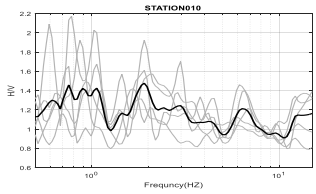

Figure 8. Site effect of station 010

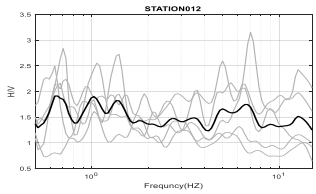

Figure 9. Site effect of station 012

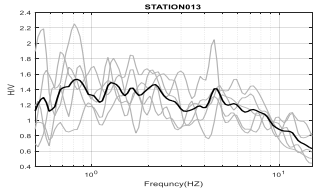

Figure 10. Site effect of station 013

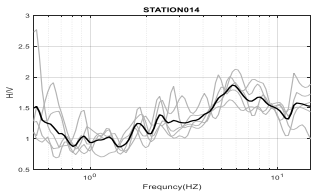

Figure 11. Site effect of station 014

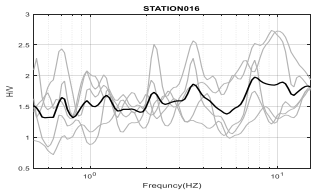

Figure 12. Site effect of station 016

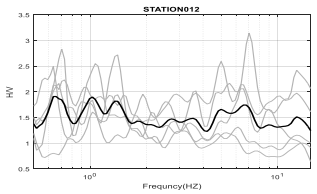

Figure 13. Site effect of station 102

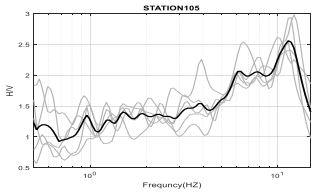

Figure 14. Site effect of station 105

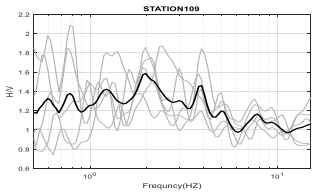

Figure 15. Site effect of station 109

Table 1 shows the results of the evaluation of the site effect.

Table 1. Results of the site effect of the studied stations based on Geopsy and MATLAB software.

Station Name	Soil Amplification Fault	Frequency (HZ)
001	2.8834	1.9267
003	0.5	3.0572
006	4.0655	2.0773
007	0.7551	3.1194
008	3.9282	2.0083
010	1.9093	1.4768
012	0.6582	1.9101

013	0.8371	1.5323
014	5.7322	1.8681
016	7.5454	1.9772
102	0.5543	2.3555
105	11.3954	2.5601
109	1.976	1.5863

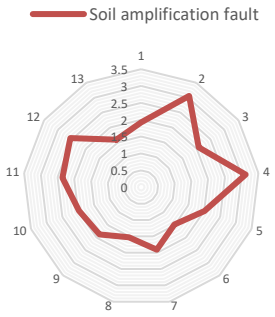

Figure 16. Site effects of the stations

5 ANALYSIS

We used simulation of the strong motions of possible earthquakes in Tehran using the finite fault modeling; In this study, the EXSIM program was used to Prediction of strong ground motion for the possible scenario of Tehran earthquake caused by Mosha fault. Regarding the fact that the amount of the slip distribution and asperity model on the fault were not available, we used this program to evaluate the slip distribution randomly. Other parameters of this program are shown in table 2. Considering this model's parameters, the simulation of Tehran earthquake strong ground motion was done by the finite fault method. In this study, the dimensions of the fault for the Tehran earthquake were determined to be are 78km in length, along the rupture and its width is 23km. The fault plate which causes the earthquake is supposed to be strike 281 degrees with a dip of 70 degrees. Its stress drop is 130 bars (Motazedian 2006).

Table 2 EXSIM parameters for Mosha fault (Motazedian 2006)

Fault Orientation Strike	Strike 281°; Dip 70°
Kappa Factor (High-Cut Filter)	0.05
Shear Wave Velocity	3.6 km/s
Crustal Density	2.8 g/cm^3
Fault Length	78km
Fault Width	23km
Stress Drop (Bars)	130 bars
Anelastic Attenuation; Q (F)	$87\ f^{0.94}$
Geometric Spreading	$\begin{cases} \frac{1}{R} & R < 70Km \\ R^{0.2} & 70Km < R < 150Km \\ \frac{1}{R^{0.1}} & R > 150Km \end{cases}$
Distance Dependent Duration	$T_0 + 0.09R$
Rupture Velocity	0.8 x share wave velocity
Windowing Function	Saragoni-Hart
Slip Distribution	Random
Moment Magnitude	7.3
Sub-Fault Dimension	2 by 2 km

The outputs of the EXSIM program have been depicted in the form of acceleration time series and Fourier semi logarithmic for each station

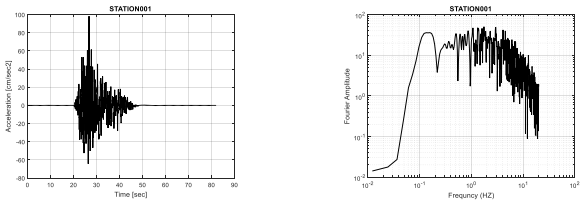

(a) strong motion (b) Fourier transform

Figure 17. strong motion and semi-logarithmic frequency spectrum with Fourier transform of station 001.

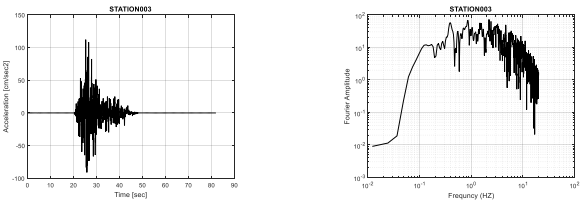

(a) strong motion (b) Fourier transform

Figure 18. strong motion and semi-logarithmic frequency spectrum with Fourier transform of station 003.

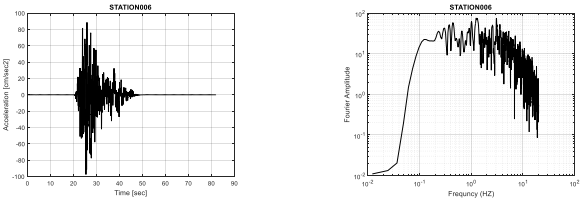

(a) strong motion (b) Fourier transform

Figure 19. strong motion and semi-logarithmic frequency spectrum with Fourier transform of station 006.

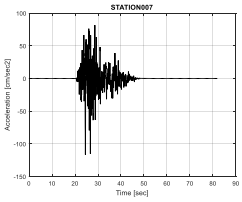

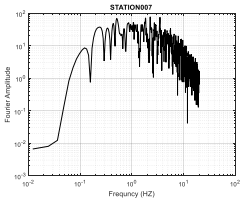

(a) strong motion (b) Fourier transform

Figure 20. strong motion and semi-logarithmic frequency spectrum with Fourier transform of station 007.

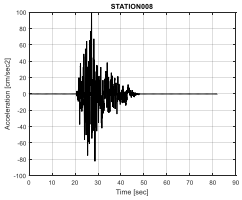

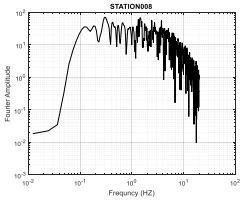

(a) strong motion (b) Fourier transform

Figure 21. strong motion and semi-logarithmic frequency spectrum with Fourier transform of station 008.

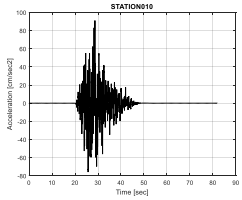

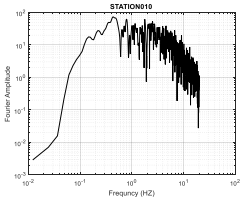

(a) strong motion (b) Fourier transform

Figure 22 strong motion and semi-logarithmic frequency spectrum with Fourier transform of station 010.

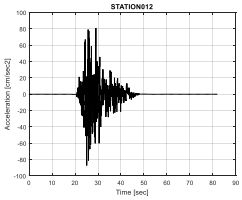

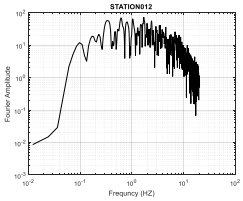

(a) strong motion (b) Fourier transform

Figure 23. strong motion and semi-logarithmic frequency spectrum with Fourier transform of station 012.

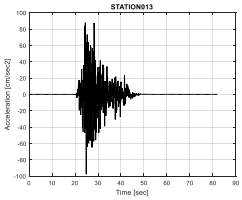

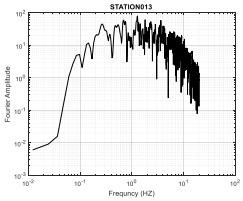

(a) strong motion (b) Fourier transform

Figure 24 strong motion and semi-logarithmic frequency spectrum with Fourier transform of station 013

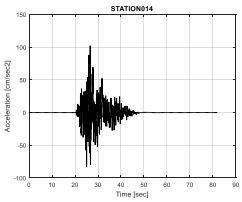

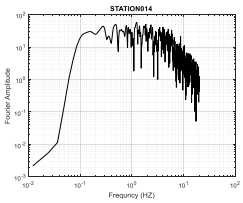

(a) strong motion (b) Fourier transform

Figure 25. strong motion and semi-logarithmic frequency spectrum with Fourier transform of station 014.

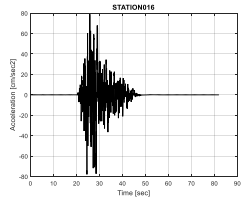

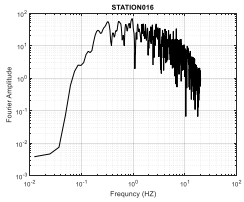

(a) strong motion (b) Fourier transform

Figure 26. strong motion and semi-logarithmic frequency spectrum with Fourier transform of station 016.

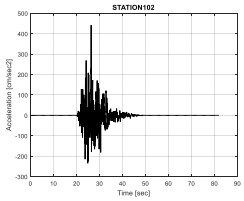

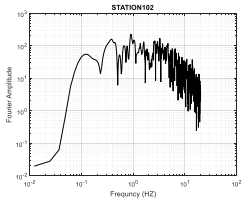

(a) strong motion (b) Fourier transform

Figure 27. strong motion and semi-logarithmic frequency spectrum with Fourier transform of station 102.

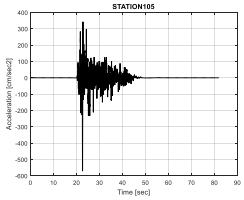

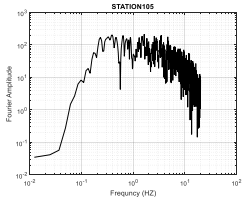

(a) strong motion (b) Fourier transform

Figure 28. strong motion and semi-logarithmic frequency spectrum with Fourier transform of station 105.

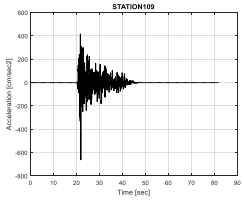

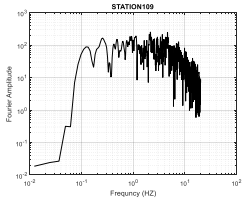

(a) strong motion (b) Fourier transform

Figure 29**.** strong motion and semi-logarithmic frequency spectrum with Fourier transform of station 109.

The strong ground motion outputs of EXSIM program are depicted in figure 30 and figure 31 on the map of Tehran and table 3.

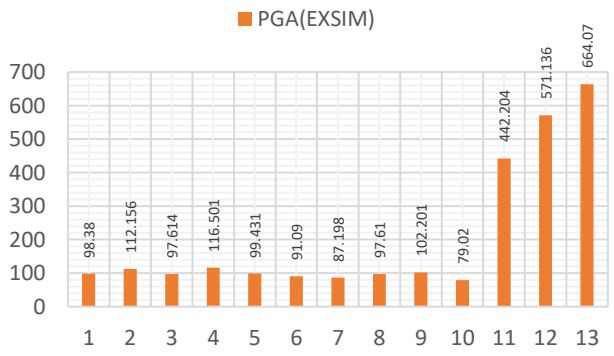

Figure 30. The bar chart of the strong motion outputs

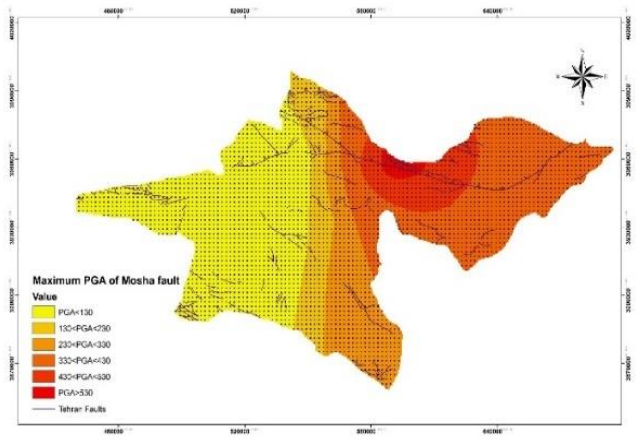

Fig. 31 distributed strong motion from EXSIM program in Tehran city

Table 3 shows the results of EXSIM outputs.

Table 3. The results of EXSIM outputs

Station Name	Latitude	Longitude	H/V	Frequency (HZ)	PGA-EXSIM(CM/S2)
001	35.74	51.36	1.9267	2.8834	98.38 $\frac{cm}{s^2}$
003	35.8	51.4	3.0572	0.5	112.156 $\frac{cm}{s^2}$
006	35.74	51.5	2.0773	4.0655	97.614 $\frac{cm}{s^2}$
007	35.76	51.39	3.1194	0.7551	116.501 $\frac{cm}{s^2}$
008	35.65	51.4	2.0083	3.9282	99/431 $\frac{cm}{s^2}$
010	35.59	51.43	1.4768	1.9093	91.09 $\frac{cm}{s^2}$
012	35.68	51.41	1.9101	0.6582	87.198 $\frac{cm}{s^2}$
013	35.76	51.41	1.5323	0.8371	97.61$\frac{cm}{s^2}$
014	35.72	51.38	1.8681	5.7322	102.201$\frac{cm}{s^2}$
016	35.75	51.28	1.9772	7.5454	79.02 $\frac{cm}{s^2}$
102	35.73	51.85	2.3555	0.5543	442.204 $\frac{cm}{s^2}$
105	35.72	52.06	2.5601	11.3954	571.136 $\frac{cm}{s^2}$
109	35.76	52.05	1.5863	1.976	664.07 $\frac{cm}{s^2}$

6 RESULTS AND DISCUSSION

In order to validate and confirm the strong ground motion of finite fault method by EXSIM program, we used two methods to compare the produced strong ground motion.

6.1 *statistical comparison with Ambraseys attenuation relationship*

Comparing the range of the greatest ground motion of attenuation relationship (Ambraseys, Simpson et al. 1996), table 4 shows that the simulated parameters of this research have a meaningful overlap in almost all of the stations.

To generate the strong ground motions by Ambraseys attenuation relationship method, we use the following formula; We get the amounts of the parameters of this formula from the Ambraseys table (Ambraseys, Simpson et al. 1996) to calculate the PGA of each station with Eq. (6).

$$logy = a_1 + a_2 M_w + (a_3 + a_4 M_w) \times log\sqrt{d^2 + a_5^2} + a_6 s_S + a_7 s_A + a_8 F_N + a_9 F_T + a_{10} F_O \quad (6)$$

S_S=soft soil sites s_A=stiff soil sites F_N=normal faulting earthquakes F_T=thrust faulting earthquakes F_O=odd faulting earthquakes

Table 4. Output of Ambraseys attenuation relationship

Name station	PGA(Ambraseys)
1	276 cm/s^2
3	301 cm/s^2
6	312 cm/s^2
7	300 cm/s^2
8	296 cm/s^2
10	204 cm/s^2
12	283 cm/s^2
13	201 cm/s^2
14	234 cm/s^2
16	264 cm/s^2
102	389 cm/s^2
105	462 cm/s^2
109	328 cm/s^2

Ambraseys attenuation relationship is one of the formulas used for attenuation relationship. Figs. 32-33 compares the Ambraseys attenuation relationship and the produced strong motions and the form of the comparison of the Ambraseys attenuation relationship strong motion in the stations. The table 5 which compares the stations is presented.

Figure 33. Comparing the Acceleration in EXSIM and Ambraseys attenuation relationship

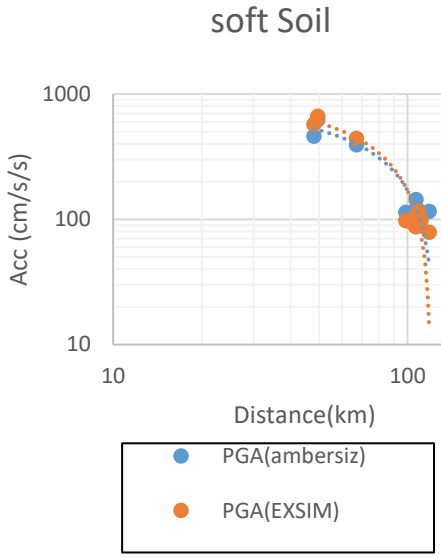

Figure 33. Comparing the produced strong motion in EXSIM and Ambraseys attenuation relationship

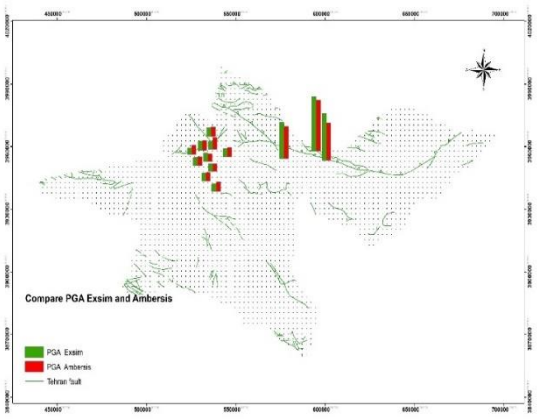

Table 5: Comparing the simulated PGA by Ambraseys formula and EXSIM program

Station Name	$(PGA\ (EXSIM))$ $/(PGA\ (AMBRASEYS))$
001	0.894925045
003	0.953601037
006	0.859796714
007	0.981827934
008	0.960597312
010	0.785097764
012	0.972214024
013	0.679628432
014	1.080802192
016	0.682115434
102	1.124968272
105	1.240760677
109	1.067641895

6.2 *Comparing the produced strong motion with the real strong motion*

3 stations studied for producing artificial strong motion for Mosha fault are similar to the stations, recorded October 17, 2009, Shahr-e Rey earthquake, which is the only authentic recorded earthquake in Tehran, measuring Mw = 4.2 and 20km depth, in 35-57 northern latitude and 51-57 eastern longitude interval. We then considered them equivalent to each other and compared the real generated data with our artificially generated data to calculate Fourier Transform and Spectrum Analysis and the response spectrum.

6.2.1 *Methodology*

First, considering the recorded data obtained from the Iran Strong Motion Network, Road, Housing and Urban Development Research Center (BHRC) (Strong Motion Network 2018) for these three stations, we evaluate Acceleration, spectrum response, and the semi logarithmic Fourier transform. Then, using the EXSIM program, we produce artificial strong ground motions for these three stations and investigate the results.

Geographical coordinates of 008 station for artificial strong ground motion for Mosha fault is very similar to the Shar-e Ray earthquake "Tehran 13" station; we compared these two with each other.

Table 6: Geographic coordinates of studied stations

Station Name	Latitude	Longitude
Tehran 13	35.647	51.397
008	35.65	51.4

These stations (Tehran 13 and 008) have similar features and different coordinates, but we considered them as one station. The 001 and 010 stations, which were tested by an artificial strong motion simulation, have exactly the same features and overlaps with Shar-e Ray earthquake stations. Table 7 shows the results.

Table 7: Comparing the PGA of real stations and simulated EXSIM program

Station Name	PGA (BHRC)	PGA (EXSIM)	$(PGA\ (BHRC))$ $/(PGA\ (EXSIM))$
Tehran 13-008	$10.97 cm/s^2$	$8.25\ cm/s^2$	1.32969697
001	$7.72\ cm/s^2$	$6.6\ cm/s^2$	1.169697
010	$16.7\ cm/s^2$	$16.65\ cm/s^2$	1.003003003

The existing difference in Tehran 13 and 008 stations are due to the fact that they don't have the exact coordinates, but the results are perfectly aligned with each other in the 001 and 010 stations.

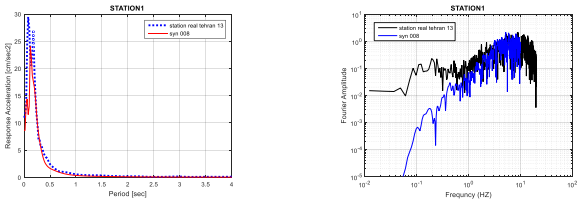

Fig 34. Comparing the real and artificial response spectrum record (left) and semi logarithm record (right) of Tehran13 (real data) and the 008 stations (artificially generated data).

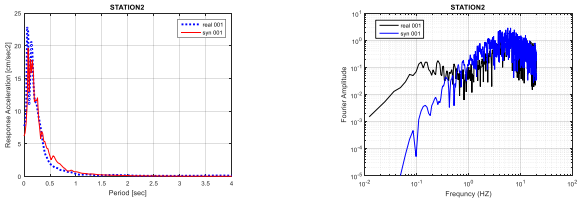

Fig 35. Comparing the real and artificial response spectrum record (left) and semi logarithm record (right) of 001 station.

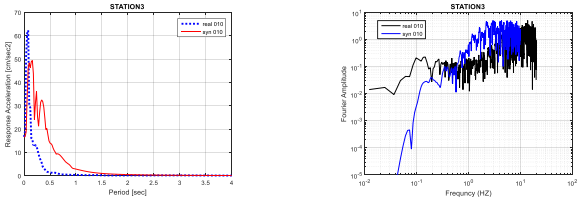

Fig 36. Comparing the real and artificial response spectrum record (left) and semi logarithm record (right) 010 station.

7 CONCLUSIONS

Considering the fact that in both Ambraseys attenuation relationship and the real strong motion in the stations we had meaningful results, we can state that the generated strong motion for Mosha fault in 13 stations in Tehran were almost precise and it can be inferred that the range of the biggest PGA belongs to the 109 station in the eastern part of the Tehran which is 664.07 cm/s^2 and the lowest PGA belongs to the 012 station which is 87.198 cm/s^2. Generally, the volume of acceleration distribution in Tehran city for Mosha fault is 87.198 cm/s^2 to 664.07 cm/s^2. Accordingly, fundamental studies for reducing the hazardous events and the risk of the earthquakes caused by Mosha fault in Tehran, east of Tehran in particular, gives the impression to be of high importance.

8 REFERENCES

Allenbach, P., "Geologie und Petrographie des Damavand und Seiner Umgeburg (Zentral Elburz), Iran", ETH Zürich, Zurich, Switzerland, 1966.

Ambraseys, N. N, Simpson, K. A. and Bommer, J. J., "Prediction of Horizontal Response Spectra in Europe, Earthquake Engineering and Structural Dynamics", Earthquake Eng. Struct. Dyn., Vol. 25, No. 4, 1996, pp. 371-400.

Anderson, J., and Hough S.E., "A model for the shape of the Fourier amplitude spectrum of acceleration at high frequencies", Bull. Seism.Soc.Am. Vol. 74, No. 5, 1982, pp. 1969-1993.

Assereto, R., "Explanatory Notes on The Geological Map of Upper Djadjerud and Lar Valleys (Central Elburz, Iran), Scale 1:50.000", Institute of Geology of the University of Milan, Milan, Italy, 1966.

Berberian, M., "Natural Hazards and The First Earthquake Catalogue of Iran: Historical Hazards in Iran Prior to 1900", IIEES, Tehran, Iran, 1994.

Boore, D. M., "Simulation of ground motion using the stochastic method", pure and applied geophysics, Vol. 160, No. 3-4, 2003, pp. 635–676.

Dellenbach, J., "Contribution a L'étude Géologique de la Régionsituée à L'est de Teheran (Iran) ", University of Strasbourg, Strasbourg, France, 1964.

Hartzell, S., "Earthquake aftershocks as Green's functions", Geophys. Res. Lett. Vol. 5, No. 1, 1978, pp. 1–14.

Mavroeidis, G. P. and Papageorgiou, A. S., "A mathematical representation of near-fault ground motions", Bull. Seism. Soc. Am. Vol. 93, No. 3, 2003, pp. 1099-1131.

Motazedian, D., "Region-Specific Key Seismic Parameters for Earthquakes in Northern Iran", Bull. Seism. Soc. Am. Vol. 96, No. 4A, 2006, pp. 1383-1395.

Motazedian, D., and Atkinson, G. M., "Stochastic Finite Fault Modeling Based on a Dynamic Corner Frequency", B. Seismol. Soc. Am., Vol. 95, No. 3, 2005, pp. 995-1010.

Nakamura, Y., "A method for dynamic characteristics estimation of subsurface using microtremor on the ground surface", QR RTRI., Vol 30, No. 1, 1989, pp. 25–33.

Statistical Center, "Statistical Center of Iran, Plan and Budget Organization", Tehran, Iran, 2018, https://www.amar.org.ir/.

Strong Motion Network, "Iran Strong Motion Network, Road, Housing and Urban Development Research Center", Tehran, Iran, 2018, https://ismn.bhrc.ac.ir/.

Tatar, M., Hatzfeld, D., Abbassi, A., and Fard, F. Y., "Microseismicity and seismotectonics around the Mosha fault (Central Alborz, Iran) ", Tectonophysics, Vol. 544–545, 2012, PP. 50-59.

Tchalenko, J. S., and Braud, J., "Seismicity and structure of the Zagros (Iran): The Main Recent Fault between 33o and 35oN", Phil. Trans. R. Soc. Lond., A., Vol. 227, No. 1262, 1974, pp. 1-25.

Wells, D. and Coppersmith, K., "New empirical relationships among magnitude, rupture length, rupture width, rupture area, and surface displacement", Bull. Seism. Soc. Am., Vol. 84, No. 4, 1994, pp. 974–1002.